Single Turnover EPR Studies of Benzoyl-CoA Reductase[†,‡]

Matthias Boll,*[,§] Georg Fuchs,[||] and David J. Lowe[§]

Institut für Biologie II, Universitat Freiburg, Schänzlestrasse 1, D-79104 Freiburg, Germany

Received December 6, 2000

ABSTRACT: Benzoyl-CoA reductase (BCR) catalyzes the ATP-driven transport of two electrons from a reduced 2[4Fe-4S] ferredoxin to the aromatic ring of benzoyl-CoA. A mechanism involving radical species and very low potential electrons similar to the Birch reduction of aromatics has been suggested for this reaction. The redox centers of BCR have previously been identified, by EPR- and Mössbauer spectroscopy, to be three cysteine-ligated [4Fe-4S] clusters [Boll et al. (2000) *J. Biol. Chem. 275*, 31857−31868] with redox potentials more negative than −500 mV. In this work, the catalytic cycle of BCR was studied by freeze−quench experiments; the dithionite reduced enzyme was rapidly mixed with equimolar amounts of benzoyl-CoA and excess MgATP plus dithionite, and subjected to EPR spectroscopic analysis. The turnover period of the enzyme under the conditions used was 3 s. The total $S = {}^1/_2$ spin concentration increased 3-fold very rapidly (within ∼25 ms). In the course of a single turnover the extent of enzyme reduction decreased again, finally reaching the starting value. An increased magnetic interaction of [4Fe-4S] clusters and the rise of an $S = {}^7/_2$ high-spin EPR signal occurred as second simultaneous and transient events (at ∼200 ms). Previous work showed that binding of the nucleotide affects the magnetic interaction of [4Fe-4S] clusters, whereas hydrolysis of MgATP is required for the switch to high-spin EPR signals. Finally, two novel transient EPR signals with an isotropic line-shape developed maximally in the late phase of the catalytic cycle (∼1−2 s). These signals differed from those of typical free radicals by shifted g values at $g = 2.015$ and $g = 2.033$ and by an unusually fast relaxation rate, suggesting an interaction of these paramagnetic species with $[4Fe\text{-}4S]^{+1}$ clusters. On the basis of these results, we present a proposal for a catalytic cycle involving radical species.

Benzoyl-CoA reductase (BCR)[1] is a central enzyme of anaerobic aromatic metabolism catalyzing the two-electron reduction of benzoyl-CoA to cyclohexa-1,5-diene-1-carbonyl-CoA by reduced ferredoxin (*1*−*6*). The two-electron transfer from reduced ferredoxin to the aromatic ring is stoichiometrically coupled to the hydrolysis of two molecules of MgATP to MgADP + Pi (Figure 1A) (*4*). This feature of BCR is analogous to nitrogenase although the two enzymes have different molecular architectures. A radical mechanism of alternate one-electron and one-proton-transfer steps to the aromatic ring has been proposed for the BCR reaction (*3*, *7*). The proposed reaction mechanism comprises the following steps: (i) electron transfer to the aromatic ring affording a radical anion, (ii) protonation to the free radical, (iii) transfer of a second electron yielding an anion, and (iv) a second protonation to a diene (Figure 1B). The mechanism is considered to be analogous to the Birch reduction in chemistry (*8*). A ketyl radical anion is suggested to be the first intermediate (*7*). A high redox barrier has to be overcome, since the transfer of the first electron to a thioester of benzoic acid requires a potential of −1.9 V (*5*). It has been suggested that a partial protonation of the substrate could make the redox potential of the first reduction step substantially more positive (*5*).

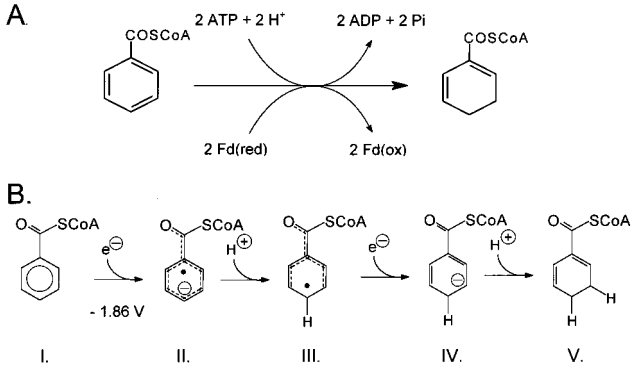

FIGURE 1: Reaction catalyzed by benzoyl-CoA reductase and the Birch reduction of benzoyl-CoA. (A) Reaction catalyzed by BCR. (B) Birch mechanism of benzoyl-CoA reduction. (I) Benzoyl-CoA, (II) radical anion, (III) neutral radical, (IV) anion, and (V) cyclic conjugated 1,5-diene.

The enzyme has only been purified so far from the denitrifying bacterium *Thauera aromatica* when grown anaerobically on an aromatic substrate and nitrate (*4*). The 163 kDa enzyme consists of four different subunits with molecular masses of 49, 48, 44, and 29 kDa as deduced from

[†] This work was supported by grants from the EC BIOTECH program, the Deutsche Forschungsgemeinschaft, the Fonds der Chemischen Industrie and the BBSRC.

[‡] Dedicated to Professor Wolfgang Buckel, University of Marburg, on the occasion of his 60th birthday.

* To whom correspondence should be addressed. Fax: +49-761-2032626. Phone: +49-761-2032685. E-mail: boll@uni-freiburg.de.

[§] Biological Chemistry Department, John Innes Centre, Colney, Norwich NR4 7UH, U.K.

[||] Institut für Biologie II, Mikrobiologie, Universität Freiburg, Schänzlestr.1, D-79104 Freiburg.

[1] BCR, benzoyl-CoA reductase; Ado*PP*[NH]*P* adenosine 5′[β,γ-imido]triphosphate; Mops, 4-morpholinopropanesulfonic acid.

10.1021/bi002771l CCC: $20.00
Published on Web 06/01/2001

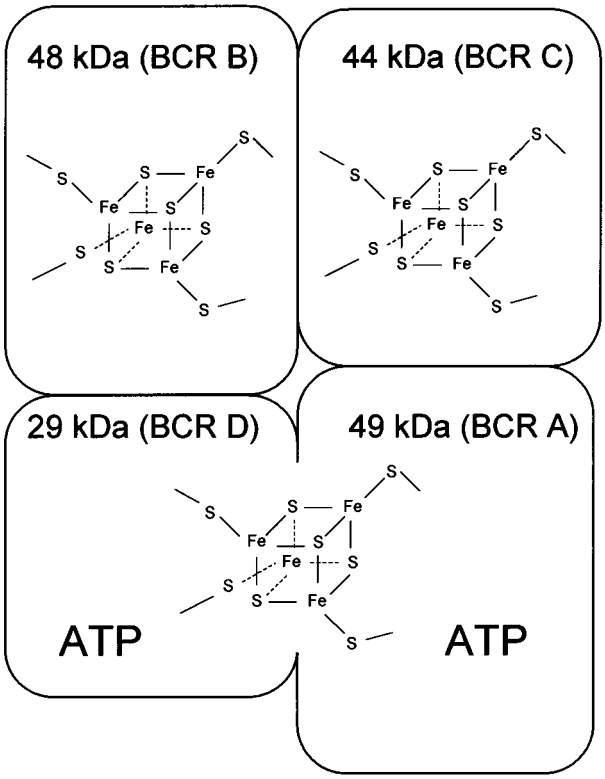

FIGURE 2: Model of the molecular composition of BCR. The ATP-binding sites are deduced from sugar kinase-type ATP-binding motifs in the α- and δ-subunit of the enzyme. One [4Fe-4S] cluster is ligated by two cysteines of each of the 29 and 49 kDa subunit.

the amino acid sequence (*9*). It contains 10−12 mol/mol of both iron and acid-labile sulfur. In a previous study the nature of the metal centers of BCR were identified by electron paramagnetic resonance (EPR) and Mössbauer spectroscopy as three cysteine-ligated $[4Fe\text{-}4S]^{+1/+2}$ clusters, referred to as clusters I−III (*10*). High sequence similarities with other ATP-dependent electron activating enzymes from amino acid fermenting clostridia suggested that one [4Fe-4S] cluster is located at the interface of the 49 and 29 kDa subunits and is ligated by two cysteines of each of the subunits (*10*, *11*). These two subunits each contain one ATP-binding site and are considered to comprise an ATP-dependent electron activating module referred to as activase (*11*). The 44 and 48 kDa subunits are proposed to be the aromatic substrate binding and reducing site harboring the other two [4Fe-4S] clusters (Figure 2).

Reduced BCR also exhibits an ATP hydrolyzing activity when benzoyl-CoA is absent; this activity is 15% of that in the presence of benzoyl-CoA. This ATPase activity is lost upon mild oxidation of the enzyme and can be reversibly switched on by reduction of the enzyme, indicating that the redox state of the enzyme modulates this activity (*12*). Under steady-state conditions of this ATPase activity two major effects have been observed: first, a decoupling of magnetically interacting $[4Fe\text{-}4S]^{+1}$ clusters and second, a switch from the $S = {}^1/_2$ to the $S = {}^7/_2$ state of one or more $[4Fe\text{-}4S]^{+1}$ cluster (*10*, *12*). The first effect was also induced by the nonhydrolyzable ATP analogue Ado*PP*[NH]*P* indicating that binding of the nucleotide was sufficient to effect the magnetic interaction of clusters. However, the switch to the unusual $S = {}^7/_2$ state of [4Fe-4S] cluster(s) depended strictly on the presence of ATP-hydrolytic activity.

To explore successive events in the catalytic cycle of BCR, we studied the EPR properties of dithionite-reduced enzyme in single turnover freeze-quench experiments. Our goal was to follow the transfer of electrons from dithionite via the previously detected and characterized [4Fe-4S] centers to the substrate. In addition we investigated the time-dependence of ATP-induced changes: the rise of the $S = {}^7/_2$ EPR signals and the proposed reversible magnetic interaction of [4Fe-4S] clusters. Finally, we also searched for novel EPR signals, such as might be given by free radical species, under pre-steady-state conditions. There is as yet no spectroscopic evidence for a mechanism involving radical formation during enzymatic ring reduction.

EXPERIMENTAL PROCEDURES

Growth of Bacterial Cells. T. aromatica was isolated in our laboratory and has been deposited in the Deutsche Sammlung von Mikroorganismen (Braunschweig, Germany; DSM 6984) (*13*). It was grown anoxically at 28 °C in a mineral salt medium in a 200 l fermenter; 4-OH-benzoate and nitrate in a molar ratio of 1:3.5 served as sole sources of energy and cell carbon. Continuous feeding of the substrates, cell harvesting, and storage and preparation of cell extracts, were carried out as described elsewhere (*14*).

Protein Purification, Enzyme Activity Assay, Purity Control and Sample Storage. Purification of BCR from extracts of *T. aromatica* was performed under strictly anaerobic conditions in a glovebox under a N_2/H_2 atmosphere (95:5, by vol.) as described earlier (*4*). Concentration of the protein samples was achieved by centrifugation (8000*g*) in Microsep Microconcentrators (exclusion limit 50 kDa). The concentration of the enzyme was 50−60 mg mL^{-1} for freeze−quench experiments. The purity of these enzyme preparations was >90% as estimated by Coomassie staining of SDS−PAGE gels. In previous experiments we have shown that an additional chromatography step using a Mono Q anion exchange column (Pharmacia) increased the purity up to virtual homogeneity but did not increase the specific activity of the enzyme indicating a concomitant loss of activity. This purification step was therefore omitted, giving 90−95% pure enzyme. In control experiments, we showed that no paramagnetic species were present in the impurities. Enzyme activity was determined in a continuous spectrophotometric assay using reduced methyl viologen as electron donor. The benzoyl-CoA and MgATP dependent oxidation of reduced methyl viologen was recorded at $\lambda = 730$ nm ($\epsilon_{730} = 2.4$ mM^{-1} cm^{-1}) at 37 °C (*4*). Purified BCR (250−300 mg) was obtained from 200 g of cells (wet mass), the specific activity usually varied between 0.4 and 0.5 μmol of benzoyl-CoA min^{-1} mg^{-1}. No correlation between these variations in enzyme activity and cluster integrity has been observed. The variations are rather due to errors in protein and activity determinations as well as protein purity. Concentrated protein samples were stored anaerobically in tubes sealed with gastight stoppers at −80 °C for several months.

Freeze−Quench Experiments. Solutions for all freeze−quench experiments were prepared in an anaerobic glovebox under a 100% nitrogen atmosphere (<1.0 ppm O_2). Prior to any BCR sample preparation, excess dithionite and corresponding oxidation products were removed by passing the concentrated enzyme sample (approximately 0.5−0.6 mM;

0.5−1 mL) over a Biogel P-6 (Bio-Rad) desalting column (volume, 5 mL; diameter, 1 cm) which had been equilibrated with 150 mM Mops/KOH pH 8.3 containing 10 mM $MgCl_2$. In the freeze−quench experiments, two gastight syringes were filled anaerobically with 340 μM enzyme and 10 mM sodium dithionite (syringe one) and 10 mM MgATP, 340 μM benzoyl-CoA, and 10 mM sodium dithionite (syringe two). In control experiments, one of the substrates was omitted from syringe two. The freeze−quench equipment was carried out as described in ref *15*, where samples were rapidly frozen in isopentane at 135 K; it is not possible to recover active enzyme from the isopentane slurry since it is inactivated by residual oxygen on thawing.

EPR Spectroscopy. X-band EPR spectra were recorded on an updated Bruker 200D-SRC spectrometer. Low-temperature measurements were made using an Oxford Instruments ESR 900 cryostat modified to take sample tubes of up to 4-mm internal diameter. Recording conditions are described in the legends to the individual figures. Spin concentrations of ground-state transition EPR signals were determined by comparison with a 1.00 mM copper sulfate sample in 11 mM sodium EDTA; these concentrations were corrected for mixing between the two syringes using a packing factor of 55% (frozen solution/total volume). Due to packing inconsistencies the accuracy of the spin concentration was ±20% (*15*).

Other Methods. Benzoyl-CoA was synthesized according to Schachter and Taggart (*16*). Protein concentration was determined by the Bradford method using bovine serum albumin as standard (*17*). SDS−PAGE were performed as described by Laemmli (*18*). Protein was visualized by Coomassie blue staining (*19*).

RESULTS

General Description of Freeze−Quench Experiments. We studied the time course of EPR changes during one turnover of BCR with three different enzyme batches with quantitative differences of less than 20% between batches. A representative set of EPR spectra from one experiment recorded under various EPR conditions from enzyme samples taken in a range between 0 and 12 000 ms are presented in Figures 3−5.

The turnover number under the conditions of our experiment was 0.32 s^{-1} (pH 8.3 and 21 °C), compared with the previously reported catalytic number of 1.6 s^{-1} determined under optimal conditions (37 °C and pH 7.3). Both numbers were determined using the routine spectrophotometric assay with reduced methyl viologen as electron donor (*4*). For ease of handling, in the experiments reported here, sodium dithionite was used as reductant; this gives turnover numbers similar to those obtained with reduced methyl viologen. It is of note that the specific activity of BCR with either of these artificial reductants is approximately 3-fold lower than with the natural electron donor, a reduced 2[4Fe-4S] ferredoxin from *T. aromatica* (*6*). In control experiments, benzoyl-CoA reductase was rapidly mixed either with buffer alone, or with buffer containing only benzoyl-CoA, or buffer containing only ATP (due to a limited supply of enzyme, only one rapid-freeze time point was taken, at 24 ms, in these control experiments). In turnover experiments, BCR (340 μM) was mixed anaerobically with a solution of the same concentration of benzoyl-CoA containing an excess of

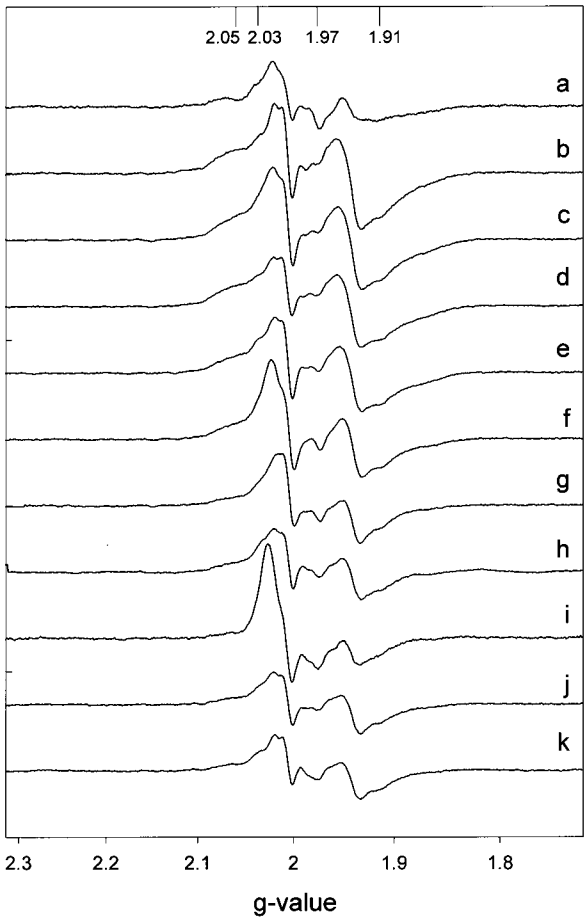

FIGURE 3: Single turnover EPR spectra of dithionite-reduced benzoyl-CoA reductase after addition of benzoyl-CoA and MgATP recorded at 18 K. BCR (340 μM) reduced by 10 mM dithionite, was then anaerobically mixed (1:1) and incubated at 21 °C for (a) 24 ms with dithionite (10 mM) containing buffer; (b−k) with dithionite (10 mM), benzoyl-CoA (340 μM) and MgATP (10 mM) containing buffer for (b) 9 ms, (c) 24 ms, (d) 42 ms, (e) 109 ms, (f) 380 ms, (g) 500 ms, (h) 1200 ms, (i) 2000 ms, (j) 3000 ms, and (k) 12000 ms. After incubation the samples were frozen in isopentane, cooled to 135 K, within 1 ms and packed into EPR tubes. EPR parameters: microwave frequency, 9.413−9.416 GHz; microwave power, 0.2 mW; modulation amplitude, 1.31 mT at 100 kHz; Temperature 18 K.

MgATP (10 mM), resulting in final concentrations, after mixing, of 170 μM both BCR and benzoyl-CoA, and 5 mM ATP. Both enzyme and substrate solutions contained 10 mM sodium dithionite in order to guarantee reducing conditions for the whole period of the freeze−quench experiment. In previous EPR studies, the same amount of dithionite was used without any indication of a loss of enzyme activity, cluster degradation or unusual dithionite dependent EPR signals (*10*, *12*). The conditions used were expected to allow one turnover, in approximately 3 s, if the reaction rate did not decrease due to the free benzoyl-CoA concentration approaching its K_M in the course of the experiment (this K_M is 15−30 μM). Since the enzyme concentration was actually comparable to that of substrate, the reaction would not be expected to follow simple Michaelis−Menten kinetics. Note that after complete consumption of benzoyl-CoA, ATP hydrolysis is expected to continue as a result of the benzoyl-CoA-independent ATPase activity of the reduced enzyme alone (*12*). The results obtained show the sequence of events in the catalytic cycle of BCR rather than provide a detailed

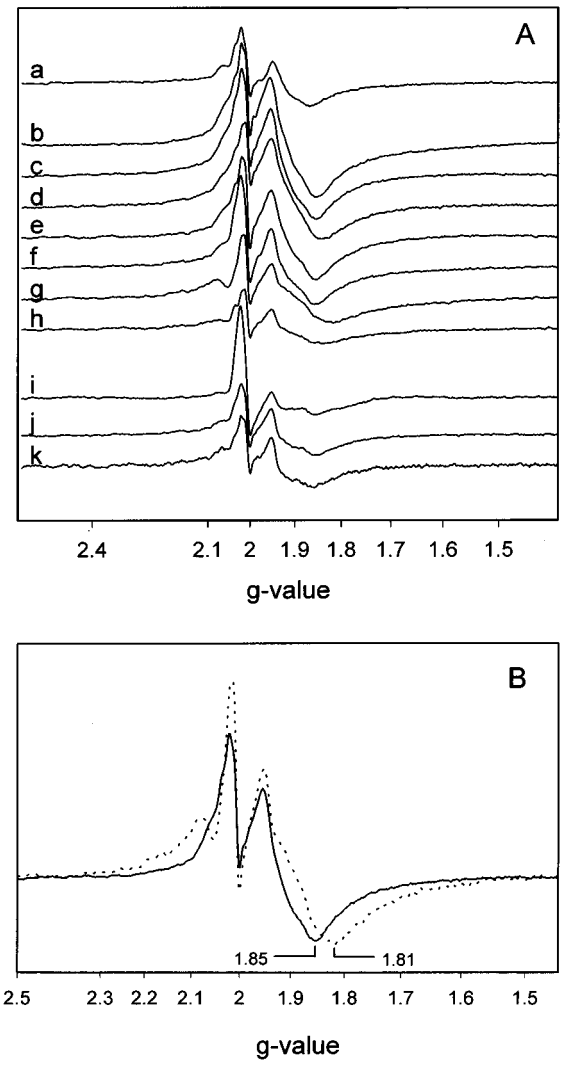

FIGURE 4: Single turnover EPR spectra of dithionite-reduced benzoyl-CoA reductase after addition of benzoyl-CoA and MgATP recorded at 4 K. (A) The samples were those of Figure 3. EPR parameters: microwave frequency, 9.413−9.415 GHz; microwave power, 0.2 mW; modulation amplitude, 1.27 mT at 100 kHz; temperature, 4 K. (B) Overlaid presentation of the EPR spectra recorded after 5 ms (—) and after 500 ms (•••) incubation of BCR with benzoyl-CoA (170 μM) and MgATP (5 mM). The arrows indicate the g values at which the signal amplitudes were determined for calculating the ratio of coupling (value obtained at $g = 1.85$)/noncoupling (value obtained at $g = 1.81$) [4Fe-4S] clusters.

kinetic study in which rate constants of all significant partial reactions are determined. The following parameters were determined in samples taken in the range 0−12 s: (i) the $S = {}^1/_2$ spin concentration of reduced [4Fe-4S] clusters at 4 and 18 K, (ii) $S = {}^1/_2$ spin concentration of $[4Fe\text{-}4S]^{+1}$ cluster II, (iii) spin concentration of $S = {}^7/_2$ high-spin species, (iv) ratio of magnetically interacting/noninteracting [4Fe-4S] clusters, and (v) the time course of the appearance and disappearance of two novel transient isotropic "radical-like" $S = {}^1/_2$ EPR signals. The sequence of these events is shown in Figure 6, which will be discussed in detail below.

$S = {}^1/_2$ $[4Fe\text{-}4S]^{+1}$ Clusters. Figure 3 shows the 18 K EPR spectra of BCR freeze−quench samples taken at various time points during the single turnover. These spectra were recorded at 2 mW microwave power where the EPR signals of noninteracting $[4Fe\text{-}4S]^{+1}$ clusters were only slightly saturated [optimal conditions are 25 K, 2 mW (*10*, *12*)], and those of interacting $[4Fe\text{-}4S]^{+1}$ clusters were not observable due to their fast relaxation. A detailed characterization of the [4Fe-4S] clusters of BCR by Mössbauer and EPR spectroscopy has been carried out previously (*10*) and gave the same g values as the present study. These were cluster I, 2.017, 1.938, 1.908; cluster II, 2.053, 1.93, 1.93; and cluster III ∼2.03, ∼1.995, ∼1.965. In the absence of benzoyl-CoA and MgATP the EPR spectrum shown in Figure 3a (0 ms-sample) displayed features from all three [4Fe-4S] clusters, including a broad feature at $g \approx 2.05$ (assigned to cluster II), and features at $g = 1.93$ and $g = 1.91$ (cluster II and I). Features around $g = 1.97$, which have been assigned to cluster III (*10*), were also observable; these are normally only detected during steady-state substrate reduction. The absolute concentration of the BCR sample before mixing with the substrates ($t = 0$ sample, Figures 3a and 6, panels A and D) was 0.7 spins/mol enzyme. A 3-fold increase of the total signal intensity (from 0.7 to 2.1 spins/enzyme) occurred in the first 24 ms after mixing the enzyme with benzoyl-CoA and MgATP (Figures 3, panels a−c, and 6A, 100% refers to the maximal reduction of all clusters in the course of our experiment, which was 2.1 spins/enzyme). The extent of substrate-induced reduction of BCR [4Fe-4S] clusters after mixing with substrate depended on the level of their reduction prior to mixing and was 1.5−3-fold. When MgATP without benzoyl-CoA was mixed rapidly (24 ms) with benzoyl-CoA reductase there was a negligible increase in cluster reduction, and on rapid mixing of enzyme with benzoyl-CoA in the absence of ATP, cluster reduction was substantially less than in the presence of both substrates (1.2−1.5-fold increase in reduction, not shown). It is therefore likely that both substrates are required for optimal electron transfer from dithionite to the [4Fe-4S] clusters of BCR. In the first 24 ms, the main effect was an increased intensity of the features at $g = 2.05$ and 1.93, which have both been assigned to cluster II (*10*). Thus the 3-fold increase in the total amount of $S = {}^1/_2$ spins is mainly caused by reduction of cluster II (>10-fold increase from 0 to 24 ms) (Figure 6A), whereas the degree of reduction of cluster III was only slightly affected. Note that the features of the cluster I EPR signal (g values at 2.017, 1.938, and 1.907) are largely superimposed on features of cluster II so that the determination of the spin concentrations of the individual clusters cannot be determined accurately under these conditions. At times from 24 ms to 2000 ms both the total and the cluster II spin concentrations decreased gradually, reaching the starting value again at 2000 ms, and subsequently remained constant (Figure 6, panels A and D). In this time range the features at $g = 1.97$ assigned to cluster III did not change significantly. In control experiments, in which BCR was mixed with buffer only before and after taking a set of freeze−quench samples, no difference in the redox state of BCR was found. BCR becomes rapidly oxidized in the absence of excess reductant even under anaerobic conditions, e.g., when passing it over a desalting column in a dithionite-free buffer. As a further control to test whether dithionite was still present at the end of an experiment, a drop of enzyme remaining in the syringe was successfully used to reduce an oxidized methyl viologen solution (1 mM in the buffer used for the freeze−quench experiment). Thus, the large excess of dithionite in the gastight syringes used was sufficient to prevent oxidation of BCR during the experiment.

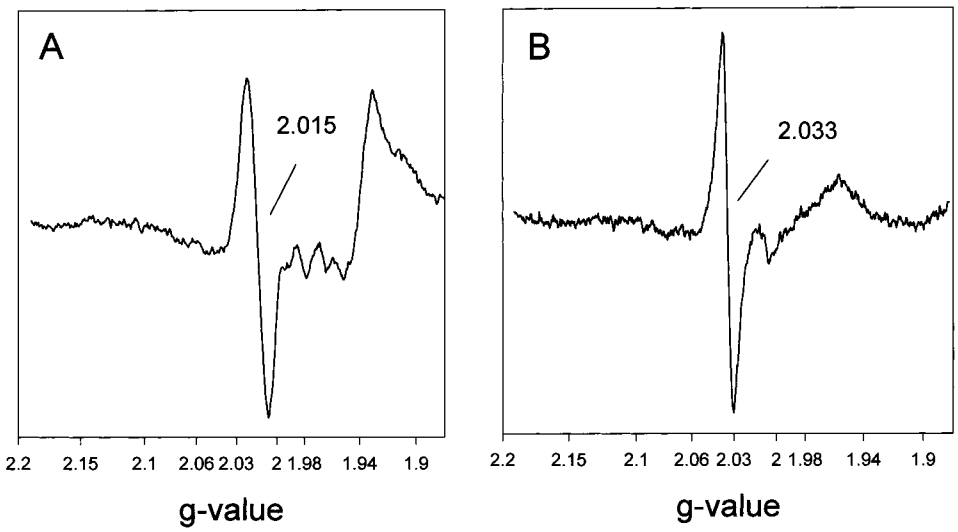

FIGURE 5: Transient "radical-like" EPR signals detected under pre-steady-state conditions of benzoyl-CoA reductase activity. (A) $g = 2.015$ signal as obtained after subtraction of the 18 K EPR spectrum of sample i of Figure 3 (after 2000 ms incubation with MgATP and benzoyl-CoA) recorded at 20 mW from the one taken at 200 mW microwave power. (B) $g = 2.03$ signal as obtained from the 4 K EPR spectrum of sample i (2000 ms) minus the 4 K EPR spectrum of sample (g) (500 ms). EPR parameters were as described in Figure 3.

$S = {}^7/_2$ [4Fe-4S]$^{+1}$ Cluster(s). In previous studies two major effects of MgATP on reduced BCR have been described: the rise of $S = {}^7/_2$ EPR signals and the reversible switch from interacting to noninteracting clusters (*10*, *12*). The $S = {}^7/_2$ high spin system observed in BCR during steady-state ATP hydrolysis has already been characterized by EPR and Mössbauer spectroscopy (*10*, *12*). It is possible to follow the switch from the low-spin to the high-spin state by the rise of two ATP-dependent EPR-signals at $g = 5.15$ and $g = 12$. To detect the time dependence of the formation of the $S = {}^7/_2$ high spin state, EPR spectra were recorded at 30 K and 20 mW from 100 to 150 mT. In this range, an isotropic EPR signal at $g = 5.15$, resulting from an excited state transition, is optimally developed (*12*). The $S = {}^7/_2$ species can be quantified relatively from the signal amplitudes alone. In a previous experiment, we determined that during steady-state ATP hydrolysis, 3.3% of the three [4Fe-4S] clusters (or 10% of a single cluster) were in the high-spin state (*10*, *12*). Comparison of the absolute signal amplitudes at $g = 5.15$ obtained in the present pre-steady-state work with those under steady state conditions in the previous study, indicated that the maximal signal amplitude (in the 500 ms sample) was 1.8 times higher than under steady-state conditions. Thus, in the 500 ms sample 6% of the three [4Fe-4S] clusters (or 18% of a single [4Fe-4S] cluster) were in the $S = {}^7/_2$ high-spin state. In the absence of MgATP no such high spin signal was observed (0 ms sample, 24 ms sample with benzoyl-CoA but without ATP). After addition of both substrates the intensity of the $S = {}^7/_2$ signal continuously increased from 0 to 500 ms and then decreased at a similar rate back to ${}^1/_3$ of its maximum value (Figure 6, panels B and E). This shows that the switch from the $S = {}^1/_2$ to the $S = {}^7/_2$ state, which has only been observed previously under steady-state conditions, is indeed a reversible process in the catalytic cycle of BCR. After all of the benzoyl-CoA had been consumed (after 3−12 s), benzoyl-CoA-independent ATPase activity started, resulting in a further doubling of the $S = {}^7/_2$ signal intensity in the samples taken at 3 s and 12 s (Figure 6E).

Interacting/Noninteracting [4Fe-4S] Clusters. In our time course experiment, we also investigated the second effect of MgATP, the reversible interaction of [4Fe-4S] clusters. The relaxation rate of the magnetically interacting [4Fe-4S] clusters is much faster than that of noninteracting clusters so that their EPR spectra are only observable at temperatures below 10 K. These signals are typically broad and featureless. To investigate this interaction, spectra were recorded at 4 K and 0.2 mW at a magnetic field between 300 and 400 mT. Under these conditions, the spectra of single clusters were saturated, so that those of the interacting clusters can be studied (Figure 4A). Notably, upon addition of both substrates (MgATP and benzoyl-CoA), the total spin concentration of magnetically interacting clusters increased rapidly to a maximum spin concentration of 1.1 spins/mol of enzyme at the same time (24 ms) as the maximum concentration of the noninteracting species. Thus, the overall spin concentration was 1.8 spins/mol of enzyme in the 24 ms sample compared to 0.6 spins/enzyme in the 0 ms sample. The line shape also changed, as demonstrated by the EPR spectra of samples taken at 9 and 500 ms shown in Figure 4B. The 500 ms sample displayed the broad spectrum of magnetically interacting clusters, whereas the 9 ms spectrum is clearly sharper, suggesting that the degree of interaction varied during the course of the experiment. To quantify the gradual transition between the interacting and noninteracting states we determined the ratio of the signal amplitudes at $g = 1.81$ and $g = 1.85$ as a measure of the ratio of interacting/noninteracting [4Fe-4S] clusters (Figure 4B). The results obtained are plotted in Figure 6, panels B and C, and show that the highest degree of interaction between [4Fe-4S] clusters was observed in the sample taken at 500 ms; this degree of interaction was taken as 100%. Interestingly, the effect of ATP hydrolysis, monitored by the rise of the $S = {}^7/_2$ signal, had a maximum value in the same sample.

Transient Isotropic $S = {}^1/_2$ Signals. One of the goals of this work was to search for spectroscopic evidence for a catalytic mechanism of BCR involving radical-containing intermediates by the detection of transient "radical-like" EPR

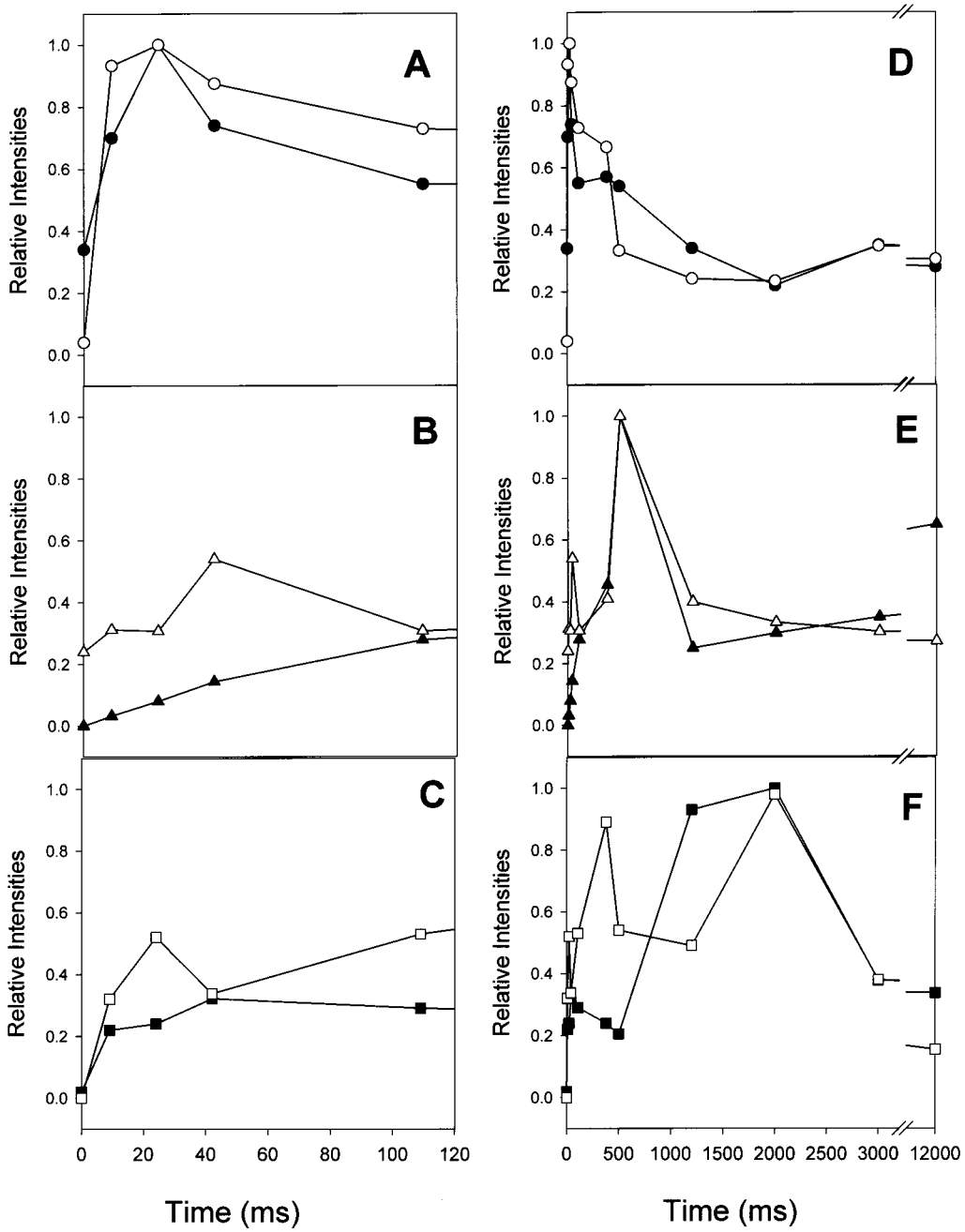

FIGURE 6: Time-dependent events in the catalytic cycle of benzoyl-CoA reductase. Reduced benzoyl-CoA reductase samples were prepared in a freeze-quench experiment as described in Figure 3. The data shown were obtained from the EPR spectra taken of samples taken after 0−12000 ms incubation of BCR (170 μM) with 5 mM MgATP and 170 μM benzoyl-CoA. 100% refers to the maximal value obtained. (A−C) show early events (0−60 ms), (D−F) show the full time scale of the freeze−quench experiment. (A and D) (●) total $S = {}^1/_2$ spin concentration determined in the 18 K EPR spectra, (○) degree of reduction of [4Fe-4S] cluster II as determined by the EPR signal amplitude at $g = 2.053$; (B and E): (△) ratio of magnetically interacting clusters/magnetically isolated clusters as determined by the ratio of the signal amplitude values at $g = 1.81$ and $g = 1.85$, (▲) relative intensity of the $S = {}^7/_2$ species; (C and F): values of the signal amplitudes of isotropic EPR signals, (□) EPR signal at $g = 2.015$ as in Figure 5A, (■) EPR signal at $g = 2.033$ as in Figure 5B. For detailed EPR conditions, see Materials and Methods and the heading to Figure 3.

signals which could be either substrate or protein derived radical species. Usually, free radicals are observed by EPR at high temperatures (up to room temperature) due to their slow relaxation rates. Typically, they exhibit an isotropic EPR spectrum around $g = 2.00$ with a narrow line width in the range between 1 and 2.0 mT. To detect such signals, EPR spectra were recorded at 80 K at 0.2 mW from the samples taken at different times. However only weak, slightly asymmetric, signals were detectable under these conditions at $g = 2.01$. Comparison with signals obtained with 100 mM dithionite containing buffer solutions gave evidence that such signals were more likely to be due to the sulfoxide radical which is in equilibrium with dithionite [not shown (*20*)]. However, in the EPR spectra recorded at 18 K (Figure 3) sharp features at $g = 2.015$ were observed which were maximally developed in the sample taken at 2000 ms (Figure 3i). A difference spectrum between this and one with low intensity (Figure 3g, 1200 ms) is presented in Figure 5A; it displays an isotropic EPR signal at $g = 2.015$ with a peak to peak distance of 2.7−3.0 mT. The optimal temperature for EPR detection of the signal was between 15 and 30 K, which is substantially lower than that typical of free radical

Table 1: Properties of the Transient EPR Signal of Benzoyl-CoA Reductase at $g = 2.033$ Observed under Pre-Steady-State Conditions of Substrate Reduction[a]

temp (K)	relative spin intensity, normalized for temperature	peak to peak width (mT)
4.1	0.87	1.27
6.6	0.94	1.25
8.5	0.98	1.17
11.0	1.00	1.08
15.0	0.35	1.05

[a] EPR conditions: microwave frequency, 9.416 GHz; microwave power, 200 mW; modulation amplitude 0.5 mT.

species. Similar normalized difference spectra were obtained between the 2000 ms spectrum and all other spectra shown in Figure 3. The rise of this isotropic signal with time, determined from the difference spectra, is shown in Figure 6, panels C and F. This plot is based on the assumption that the lowest value obtained for the signal (in the 0 ms sample) was <1% of the value obtained in the 2000 ms sample. Since pure radical species can only be observed in difference spectra from samples taken at different times, its absolute spin concentration cannot be determined accurately although a rough estimate indicated that at its maximum it accounted for 0.05−0.1 spins/enzyme (in the 2000 ms sample). No significant $g = 2.015$ signal could be detected after rapid freezing at 24 ms using only one of benzoyl-CoA or MgATP.

At very low temperatures (<15 K) and at high microwave power (>2 mW) an additional isotropic $S = {}^1/_2$ EPR signal, with a *g*-value at 2.033, was observed (Figure 5B). The peak-to-peak distance was 1.1−1.3 mT which is typical of radical species. Under the conditions used for the detection of this signal all others, except that of the interacting $[4Fe\text{-}4S]^{+1}$ clusters, were severely saturated, and the signal of the interacting clusters is too broad to obscure the sharp radical signal. At 200 mW microwave power, the normalized spin intensity decreased only slightly when the temperature was lowered from 11 to 4 K; in this temperature range only minor changes of the line width were detected (Table 1). The relative intensities as determined by the signal amplitude are plotted vs time in Figure 6, panels C and F. At 0 ms in the absence of benzoyl-CoA and ATP the signal intensity was less than 1% of the maximal value. Between 9 and 500 ms, it was 20−30% of the maximal value which was reached in the late phase of the catalytic cycle (1200−2000 ms) After benzoyl-CoA was expected to be completely exhausted, its concentration fell back to 20% of the maximal value. The maximal intensity of the $g = 2.033$ signal (referred to as 100%) was 0.007 spins/mol enzyme. Note that in the 2000 ms sample the intensities of both isotropic signals, at $g = 2.015$ and $g = 2.033$, were maximal indicating that reactions giving rise to these signals occur simultaneously.

After rapid mixing of BCR with ATP, in the absence of benzoyl-CoA, after 24 ms the concentrations of both isotropic EPR signals were less than 1% of the maximal value, whereas the $g = 2.033$ signal was 2−5% of the maximal value obtained in the 2000 ms sample at this time after mixing benzoyl-CoA with BCR in the absence of ATP. At 24 ms, in the absence of one substrate, the isotropic signal intensities were substantially less than in the presence of both (22−50% of the maximum values). However, since both radical-like signals are transients, it may be that they increase after prolonged reaction time in the absence of one of the substrates. We were unable to do extended single turnover experiments with only one substrate since, with the limited supply of enzyme we had, we chose instead to check the reproducibility of the observed effects between different batches. It is important to note that both transient isotropic EPR signals we detected were obtained with all enzyme batches in the same phase of the turnover experiment (between 1 and 2 s). The almost perfect isotropic line shape of the transient EPR signals makes it unlikely that they are given by $[3Fe\text{-}4S]^{+1}$ clusters, formed as a possible result of cluster degradation, since such clusters usually show more unsymmetrical signals. Also, the redox potential, $E'°$, of the $[3Fe\text{-}4S]^{+1/0}$ cluster of oxygen-treated BCR is ∼−100 mV which is much more positive than the redox potentials of the $[4Fe\text{-}4S]^{+1/+2}$ clusters (<−500 mV) (*12*). Thus, [3Fe-4S] clusters should be completely in the EPR silent $[3Fe\text{-}4S]^0$ state under the conditions used in the presence of dithionite. It is also most unlikely that cluster degradation is a transient and reversible process. Unfortunately, freeze-quench samples of BCR cannot be reused after the experiment since they are destroyed by residual oxygen in the isopentane upon thawing. Since control samples of BCR versus buffer taken at the beginning and end of a rapid-freeze experiments did not show significant differences, a substantial change of the redox potential in the syringes during an experiment can be excluded.

DISCUSSION

In this work, pre-steady-state events in the catalytic cycle of benzoyl-CoA reductase were studied by freeze−quench EPR spectroscopy. One goal was to establish whether the effects of the individual substrates on the EPR properties of BCR, that had previously been observed only at long times under steady-state conditions, are catalytically competent in aromatic ring reduction. Most importantly the effects of binding ATP, that causes a decoupling of magnetically interacting [4Fe-4S] clusters, and of hydrolysis of ATP, that causes a switch from the $S = {}^1/_2$ low-spin to the $S = {}^7/_2$ high-spin state of one or more $[4Fe\text{-}4S]^{+1}$ clusters, can now be assigned to events in the catalytic cycle of benzoyl-CoA reductase. Another important result of these studies was the detection of two different transient radical-like EPR signals. Benzoyl-CoA reductase is proposed to catalyze a "biological Birch reduction" of the aromatic ring involving radical species [Figure 1B (*3*, *7*)]. However, under steady-state conditions it has not been possible to assign an EPR-detectable radical to a catalytic intermediate. The data obtained in this work shed new light on the catalytic cycle of benzoyl-CoA reductase as will be discussed below where we distinguish four phases. We emphasize that all enzyme molecules are not expected to be simultaneously in identical conformations. A simplified catalytic cycle is presented in Figure 7, where each phase represents a transition between different enzyme states (panels A−D).

In phase I (0−24 ms), a rapid 2−3-fold increased reduction of the [4Fe-4S] clusters, mainly cluster II, occurred as a result of binding MgATP and benzoyl-CoA. The presence of both substrates was required for maximal enzyme reduction, so that changes in both the activase and reductase subunits must occur (see Figure 2). Such changes in the protein conformation could result in an exposure of a [4Fe-4S] cluster at the

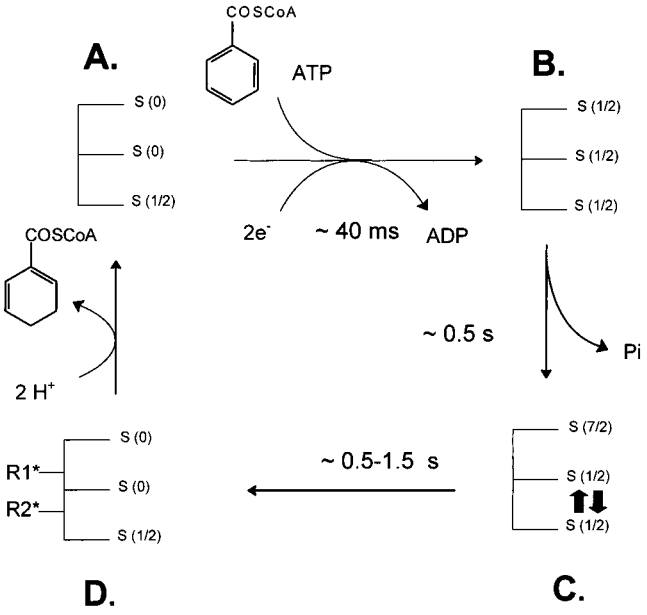

FIGURE 7: Proposed simplified catalytic cycle of benzoyl-CoA reductase. Panels A−D represent four different enzyme states. To clarify the presentation, the protein-bound substrates are omitted. Note that two electrons are transferred to the substrates in one catalytic cycle. Two ATP are hydrolyzed to ADP in the course of the reaction. The black arrows in III. represent a magnetic interaction of two $[4Fe\text{-}4S]^{+1}$ clusters, R1 and R2 represent two different radical species. The release of Pi shown in step II is intended to indicate the point in the cycle where ATP hydrolysis occurs and not necessarily where Pi dissociates from the enzyme. For further details see text.

surface of the enzyme making it more accessible to reduction by dithionite. Furthermore, cluster to cluster distances could be diminished, enabling an enhanced intramolecular electron transfer, most probably from the [4Fe-4S] cluster of the activase subunits (29 and 49 kDa) to the two [4Fe-4S] clusters of the reductase subunits (44 and 48 kDa).

Phase II (42−500 ms) is characterized by ATP-dependent effects, which are maximum in this phase and decrease again in phase III. The effect of binding (the decoupling of magnetically interacting $[4Fe\text{-}4S]^{+1}$ clusters) can qualitatively be distinguished from that of ATP hydrolysis (the switch from the $S = {}^1/_2$ to the $S = {}^7/_2$ state). Both effects have now been shown to be transient events in the catalytic cycle of BCR. Since the increase in $S = {}^7/_2$ high spin concentration and the magnetic interaction of [4Fe-4S] clusters occurred simultaneously, with both features being maximal at 500 ms, the $S = {}^7/_2$ high spin state of one [4Fe-4S] cluster appears at the same time as the magnetic interaction between two other clusters. We have shown that the magnetic interaction of [4Fe-4S] clusters and the formation of the $S = {}^7/_2$ high-spin state are reversible. Our experiments further show that in the catalytic cycle of BCR the coupling of [4Fe-4S] clusters occurs simultaneously with the formation of the $S = {}^7/_2$ high spin state, whereas the decoupling of the clusters is combined with a loss of $S = {}^7/_2$ spin intensity (Figure 6). The change from the $S = {}^1/_2$ to the $S = {}^7/_2$ state of a $[4Fe\text{-}4S]^{+}$ cluster could be a result of an ATP-hydrolysis-dependent conformational change in its vicinity that diminishes the optimal overlap of the iron and sulfur orbitals in the [4Fe-4S] cluster required for ferrimagnetic coupling of electrons. A rough theoretical estimation has indicated that at least 10−20 kJ/mol^{-1} are required for the switch from the energetically favorable $S = {}^1/_2$ state to the $S = {}^7/_2$ state of a [4Fe-4S] cluster [Meier, C., University of Lübeck; personal communication]; this energy can easily be provided by ATP hydrolysis. We were unable to detect any ATP-induced lowering of the redox potential of the [4Fe-4S] clusters since the potentials are too low to be precisely determined by redox titration experiments, and since in such experiments ATP is continuously hydrolyzed by BCR. In a preliminary cyclic voltammetry study, no direct electron transfer from pyrolytic graphite electrodes to BCR was observed (using polymyxin as promotor). It seems likely that the low potential [4Fe-4S] clusters of BCR are buried deep in the enzyme and are not accessible.

In phase III (500−2000 ms), two novel radical-like EPR signals increased to their maximum concentrations at the same time as the $S = {}^1/_2$ concentration decreased to its initial value and the $S = {}^7/_2$ concentration diminished to a minimal value. We suggest that in this late phase of the catalytic cycle, electron transfer from [4Fe-4S] cluster(s) to the substrate takes place. Both radical-like signals were only present at very low concentrations and exhibited essentially isotropic line-shapes in the $g \approx 2.0$ region and we therefore assign them to $S = {}^1/_2$ low-spin radical species of the protein and/or the substrate. Their g values are substantially shifted to lower field. We refer to the EPR signal with $g = 2.015$ as to radical R1 (with line width of 2.8 mT) and the EPR signal with $g = 2.033$ as to radical R2 (line width 1.3 mT; see Figure 5 and 7). Both reach their maximum simultaneously in the late phase of the catalytic cycle. Although substrate radicals are proposed as intermediates in the catalytic cycle of BCR any assignment of the isotropic signals obtained in this work is not yet possible. Radicals with g values >2.01 are not typical for carbon atom radical species but have been reported for sulfur radicals, e.g., thiyl radicals or disulfide radical anions which could derive from the protein (*21*, *22*). Protein derived disulfide radical anions would be an attractive candidate for such a species since the reduction potential of $R{-}S{-}S{-}R/(RS)_2^{\bullet -}$, $E'^{\circ} = -1.6$ V, has been shown to be extremely negative (*23*). A protein derived radical species could mediate electron transfer from the [4Fe-4S] cluster to the substrate. In addition to their shifted g values away from that of the free electron, these signals have unusually low temperature optima and high power saturation properties. R2 in particular exhibited extreme EPR properties since it was optimally observed at 4 K and 2 mW microwave power. We suggest that these unusual properties are a result of a strong magnetic interaction between the radical species and fast relaxing paramagnets such as the magnetically interacting [4Fe-4S] clusters of BCR which have temperature optima well below 10 K.

In phase IV (2s-12s), both radical-like signals decreased again to 15−30% of their maximal value. The enzyme returned to essentially the same state as at the beginning of the catalytic cycle, indicating that substrate reduction was essentially complete (Figures 3 and 4). The $S = {}^1/_2$ concentration reached ${}^1/_3$ of the maximal value at the end of the cycle. This fits with two electrons having been transferred to the substrate benzoyl-CoA, since benzoyl-CoA reductase contains three [4Fe-4S] clusters. At the end of the catalytic cycle in the presence of excess substrate, the products ADP and cyclohexa-1,5-diene-1-carbonyl-CoA have to exchange with ATP and benzoyl-CoA.

Summarizing the events during the individual phases, the following reaction sequence is proposed (Figure 7): (i) electron transfer to the partially oxidized BCR triggered by the binding of MgATP and benzoyl-CoA, (ii) electron "activation" by the switch of a [4Fe-4S] cluster from the low spin to the $S = {}^{7}/_{2}$ high spin state, in parallel two other clusters interact magnetically, (iii) electron transfer from the activated enzyme state to the substrate maybe via protein radical intermediates, (iv) exchange of ADP by ATP and the cyclic diene by benzoyl-CoA.

ACKNOWLEDGMENT

We thank Dr. Shirley A. Fairhurst for help with running EPR spectra and Dr. Amanda Francis for help with the preparation of the freeze−quench samples.

REFERENCES

1. Heider, J., and Fuchs, G. (1997) *Eur. J. Biochem. 243*, 577−596.
2. Harwood, C. S., Burchhardt, G., Herrmann, H., and Fuchs, G. (1999) *FEMS Microbiol. Rev. 22*, 439−458.
3. Koch, J., Eisenreich, W., Bacher, A., and Fuchs, G. (1993) *Eur. J. Biochem. 211*, 649−661.
4. Boll, M., and Fuchs, G. (1995) *Eur. J. Biochem. 234*, 921−933.
5. Boll, M., Laempe, D., Eisenreich, W., Bacher, A., Mittelberger, T., Heinze, J., and Fuchs, G. (2000) *J. Biol. Chem. 275*, 21889−21895.
6. Boll, M., and Fuchs, G. (1998) *Eur. J. Biochem. 251*, 946−954.
7. Buckel, W., and Keese, (1995) *Angew. Chem. 107*, 1595−1598.
8. Birch, A. J. (1947) *J. Chem. Soc.* 1642−1648.
9. Breese, K., Boll, M., Alt-Mörbe, J., Schägger, H., and Fuchs, G. (1998) *Eur. J. Biochem. 256*, 148−154.
10. Boll, M., Fuchs, G., Meier, C., Trautwein, A. X., and Lowe, D. J. (2000) *J. Biol. Chem. 275*, 31857−31868.
11. Hans, M., Sievers, J., Müller, U., Bill, E., Vorholt, J. A., Linder, D., and Buckel, W. (1999) *Eur. J. Biochem. 265*, 404−414.
12. Boll, M., Albracht, S. J. P., and Fuchs, G. (1997) *Eur. J. Biochem. 244*, 840−851.
13. Anders, H.-J., Kaetzke, A., Kämpfer, P., Ludwig, W., and Fuchs, G. (1995) *Int. J. Syst. Bacteriol. 45*, 327−333.
14. Brackmann, R. and Fuchs, G. (1993) *Eur. J. Biochem. 213*, 563−571.
15. Bray, R. C., Lowe, D. J., Capeillere-Blandin, C., and Fielden, E. M. (1973) *Biochem. Soc. Trans. 1*, 1067−1072.
16. Schachter, D., and Taggart, J. V. (1976) *J. Biol. Chem. 203*, 925−933.
17. Bradford, M. M. (1976) *Anal. Biochem. 72*, 248−254.
18. Laemmli, U. K. (1970) *Nature 227*, 680−685.
19. Zehr, B. D., Savin, T. J., and Hall, R. E. (1989) *Anal. Biochem, 182*, 157−159.
20. Lambeth, D. O., and Palmer, G. (1973) *J. Biol. Chem. 248*, 6095−6103.
21. Lawrence, C. C., Bennati, M., Obias, H. V., Bar, G., Griffin, R. G., and Stubbe, J. (1999*) Proc. Natl. Acad. Sci. 96*, 8979−8984.
22. Nelson, D. J., Petersen, R. L., and Symons, M. C. R. (1977) *J. Chem. Soc., Perkin Trans.* 2, 2005−2015.
23. Surdahr, P. S., and Armstrong, D. A. (1987) *J. Phys. Chem. 91*, 6532−6537.

BI002771L